Concentration dependence of the short-range order in the Ni-V and Pt-V systems

David Le Bolloc'h,[1,2,*] Alphonse Finel,[2] René Caudron[1,2]
[1]*Laboratoire Léon Brillouin, CEA-CNRS, CE Saclay, 91190 Gif sur Yvette, France*
[2]*Laboratoire d'Etude des Microstructures (LEM), ONERA-CNRS, BP72, 92322 Châtillon Cedex, France*
(Received 14 December 1999)

The short-range order (SRO) in Pt-V and Ni-V systems has been studied by diffuse scattering of neutrons over a large concentration range. In both systems, a *c*-dependent SRO has been observed. We show that this concentration sensitivity has a different origin in the two cases. In Ni-V, the change of the SRO pattern is mainly due to *c*-dependent effective pair interactions (EPI), while in Pt-V, the EPI are *c* independent. We find explicit discrepancies between our results, deduced from measurements in the *disordered* state, and the electronic structure calculations, if they are performed in the *ordered* state. These discrepancies are due to the sensitivity of the electronic structure to the state of order.

I. INTRODUCTION

Short-range order (SRO) which appears in the high temperature disordered state of alloys has been extensively studied since the SRO topology reflects the underlying interactions of the system. We report on our measurements of the SRO in two different systems, Ni-V and Pt-V, undertaken to study the concentration dependence of effective interactions and to improve our general understanding of phase diagrams.

Several theoretical studies have been devoted to the concentration dependence of the SRO in binary alloys[1,2] but few experimental works have been carried out with that perspective in mind. Experimentally, to our knowledge, the only system for which the SRO has been measured over a large concentration range is the $Ni_{1-c}Cr_c$ system,[3–5] where the SRO maxima are locked at the same $\langle 1\frac{1}{2}0\rangle$ wave-vector positions for $c=\frac{1}{3},\frac{1}{4}$, and $\frac{1}{9}$. In contrast, as we have shown in Refs. 6, 7, the topology of the SRO in the Pt-V system changes with the concentration. Despite those variations, inverse Monte Carlo simulations applied to the SRO lead to nearly *c*-independent effective pair interactions (EPI) from Pt_2V to Pt_8V. Furthermore, in order to check that this unexpected property cannot be extended to any alloy, the Ni-V system has been investigated since it looked very similar to the Pt-V system (platinum and nickel belong to the same column of the periodic table). The Ni-V and Pt-V systems display the same Pt_2Mo, DO_{22}, and A_8B (Refs. 8, 9) ordered phases on the fcc lattice. However, although the phase diagrams are similar, the interactions should be different in the two systems since the SRO maxima are not located at the same positions: Pt_3V displays maxima at the $\langle 100\rangle$ positions while in Ni_3V (Refs. 10, 11) the SRO maxima are located at the $\langle 1\frac{1}{2}0\rangle$ *q* points.

II. EXPERIMENT

All the compounds studied in this paper were grown by the Czochralsky method. Their compositions were determined by electron microprobe. To within 1%, they were consistent with the expected stoichiometries, except for Pt_8V which was found to contain 13.2% vanadium. This shift in concentration has been taken into account in the data reduction. The diffuse scattering of neutrons was performed on the spectrometer G44 at the laboratoire Léon Brillouin (CNRS/CEA), France. We followed the same procedure as outlined in Ref. 5. The (100) and (110) planes were explored *in situ*, with the incident wavelength $\lambda=2.59$ Å. In order to reject the inelastic signal due to the high population of the phonon modes at high temperature, a time of flight analysis has been used. Under these conditions the energy resolution was never greater than 4 meV. After correcting for absorption, multiple scattering and Debye-Waller attenuation, the Warren Cowley parameters $\alpha(\vec{R}_{nm})=(\langle\sigma_n\sigma_m\rangle-\langle\sigma_n\rangle\langle\sigma_m\rangle)/4c(1-c)$, and the size effect contribution were extracted from the diffuse intensity using a least square routine, based on a Sparks-Borie approach[12] for displacements, up to the first order. The results are shown in Fig. 1.

III. CONCENTRATION DEPENDENCE OF THE SRO IN PT-V AND NI-V

A. Pt-V system

From Pt_2V to Pt_8V, we observe a large effect of the concentration on the SRO topology. As with Pd_3V,[11] the diffuse intensity of Pt_3V is spread along the $\langle 1k0\rangle$ direction with maxima at the $\langle 100\rangle$ positions. These positions of the SRO maxima are not compatible with the DO_{22} ground state within the usual mean field approach. In Pt_8V, the maxima are no longer located at special points of the fcc lattice. Instead, the $\langle 100\rangle$ intensity is split along the $\langle 100\rangle$ axis and presents a saddle point (see Fig. 1). We note that these maxima are no longer located just above the superstructures of the ordered state. The Bragg peaks of the A_8B ground state are located at $\langle\frac{2}{3}00\rangle$ and $\langle\frac{2}{3}\frac{2}{3}0\rangle$ (and equivalent points), whereas the SRO intensity sits on an incommensurate *q* point, between $\langle\frac{2}{3}00\rangle$ and $\langle 100\rangle$. The Pt_4V SRO displays a topology which is intermediate between Pt_3V and Pt_8V. As Pt_3V, the maxima sit on the $\langle 100\rangle$ points (and equivalent), but the broadening of the intensity profiles along the $\langle h00\rangle$ lines is reminiscent of the Pt_8V splitting. A quite different topology has been measured in Pt_2V. The SRO maxima are located at incommensurate positions along the $\langle 1k0\rangle$ line. By symmetry, this leads to a hole at the $\langle 110\rangle$ point. Other systems such as Cu_3Zn,[13] Cu_3Au,[14,15] Cu-Pd,[16] or Cu-Al[17] display a splitting in the same direction. In Sec. IV A, we comment about the link between the incommensurate maxima of the SRO and the real space dependance of the underlying interactions.

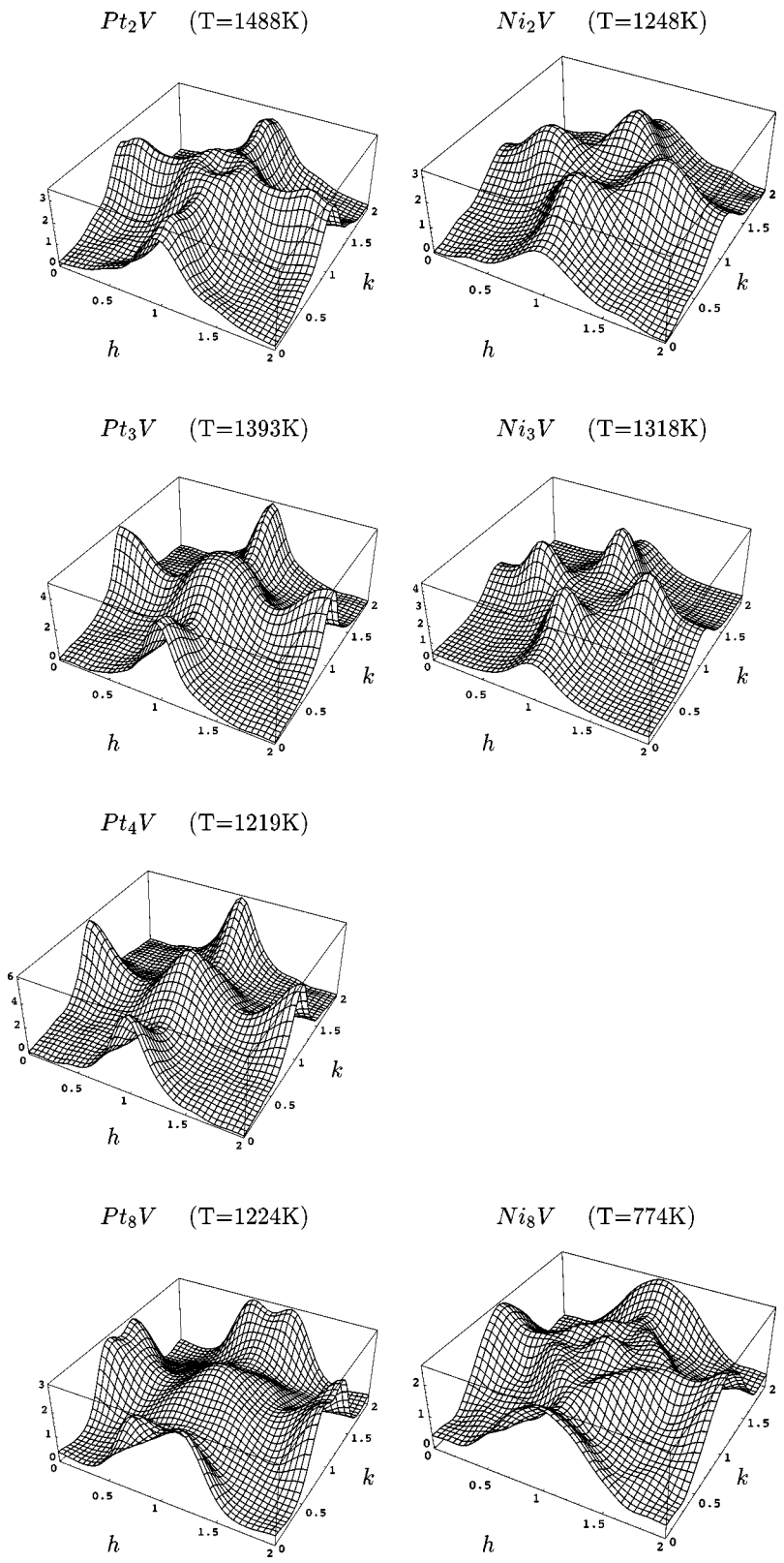

FIG. 1. Experimental short-range order in the Pt-V and Ni-V systems; (100) plane.

B. Ni-V system

In the Ni-V system, from Ni_2V to Ni_3V, the intensity maxima are locked at the $\langle 1\frac{1}{2}0\rangle$ special points but, for Ni_8V,[18] they suddenly shift to $\langle 100\rangle$. In Ni_8V, there is a broadening of the intensity profile along the $\langle h00\rangle$ direction, but, within the limit of the experimental resolution, no splitting similar to Pt_8V has been observed. That SRO evolution is more pronounced than in $Pt_{1-c}V_c$ system, for which the maxima, even if they are c-dependent, are always located in the neighborhood of the $\langle 100\rangle$ q point from $c=\frac{1}{3}$ to $c=\frac{1}{9}$.

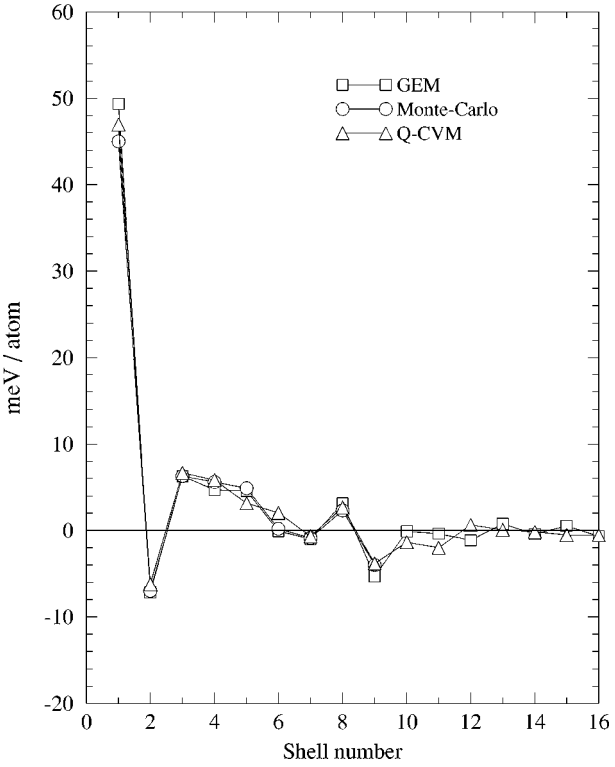

FIG. 2. EPI calculated from the Pt_3V SRO by inverse Monte Carlo simulation, inverse GEM and Q-CVM. Only the nine nearest EPI have been calculated by Monte Carlo simulation.

Notice that, in contrast to Ni_3V, the dominant wave vector of LRO and those of SRO do not coincide anymore in Ni_8V, since the A_8B phase is built on a $\frac{2}{3}\langle 110\rangle$ concentration wave.

IV. EFFECTIVE PAIR INTERACTIONS

We have interpreted the diffuse scattering using an Ising model that includes long range effective pair interactions (EPI), V_{nm}, up to the ninth neighbors $H=\frac{1}{2}\Sigma_{nm}V_{nm}\sigma_n\sigma_m + h\Sigma_n\sigma_n$, where σ_n represents the occupation variable and h the chemical potential. These EPI are not determined from *ab initio* calculations but from inverse statistical methods applied to the measured diffuse intensity maps. We have used different statistical approaches: a Monte Carlo method, the gamma expansion method (GEM) (Ref. 20) and the cluster variation method in the Q space (Q-CVM). We show in Fig. 2 the 16 first EPI obtained by the different methods and using the diffuse intensity of Pt_3V. The agreement is excellent. We would like to stress that those three methods are based on quite different approaches and assumptions. The GEM is an analytical method, the Q-CVM is a mean field approach (quasianalytical), whereas the inverse Monte Carlo is a purely numerical technique.

A set of EPI has been obtained for each of the diffuse maps of the Fig. 1 using inverse Monte Carlo simulations. The interactions are displayed on Fig. 3.

A. Concentration dependence of the EPI in Pt-V

Despite the obvious topological changes of the intensity maps, the EPI's of the Pt-V system do not depend much on concentration, except V_1. This behavior was unexpected, as

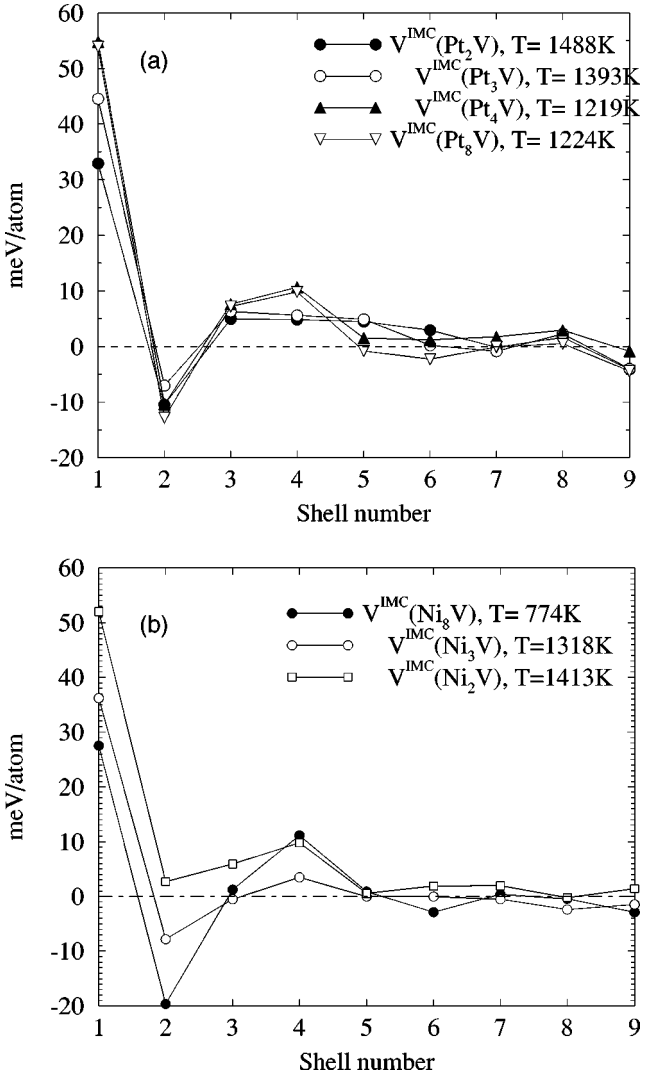

FIG. 3. Effective pair interactions in the Pt-V and Ni-V systems.

any electronic calculation must take into account the band filling, which must induce changes of the EPI. We already noticed a similarly unexpected behavior for the Ni-Cr system.[5] This weak c dependence of the interactions is confirmed by direct Monte Carlo simulations.

A single set of interactions correctly reproduces the c behavior of the SRO, from the incommensurate splitting along the $\langle 1k0\rangle$ direction in Pt_2V to the splitting along the $\langle h00\rangle$ direction in Pt_8V (Fig. 4). That strong c variation of the SRO simulated from the same interactions clearly shows that the Krivoglaz-Clapp-Moss formula[19] in insufficient. It is thus desirable to devise a simple analytical expression for $\alpha(\vec{q})$ which goes beyond the mean field KCM formula. Even though it is more accurate, the more elaborated cluster variation method is not a good candidate, as it does not provide a direct analytical link between the $V(\vec{R})$'s and the $\alpha(\vec{q})$. In the Appendix, we give a derivation of the simple analytical theory we used in our previous paper.[7] As is needed, this theory goes beyond the KCM approach. It explains the above result, i.e., how a c-dependent incommensurate SRO can be obtained from a unique set of EPI.

We now comment briefly about the link between the incommensurate maxima of $\alpha(\vec{q})$ and the real space topology of the EPI. It is often believed that an incommensurate SRO

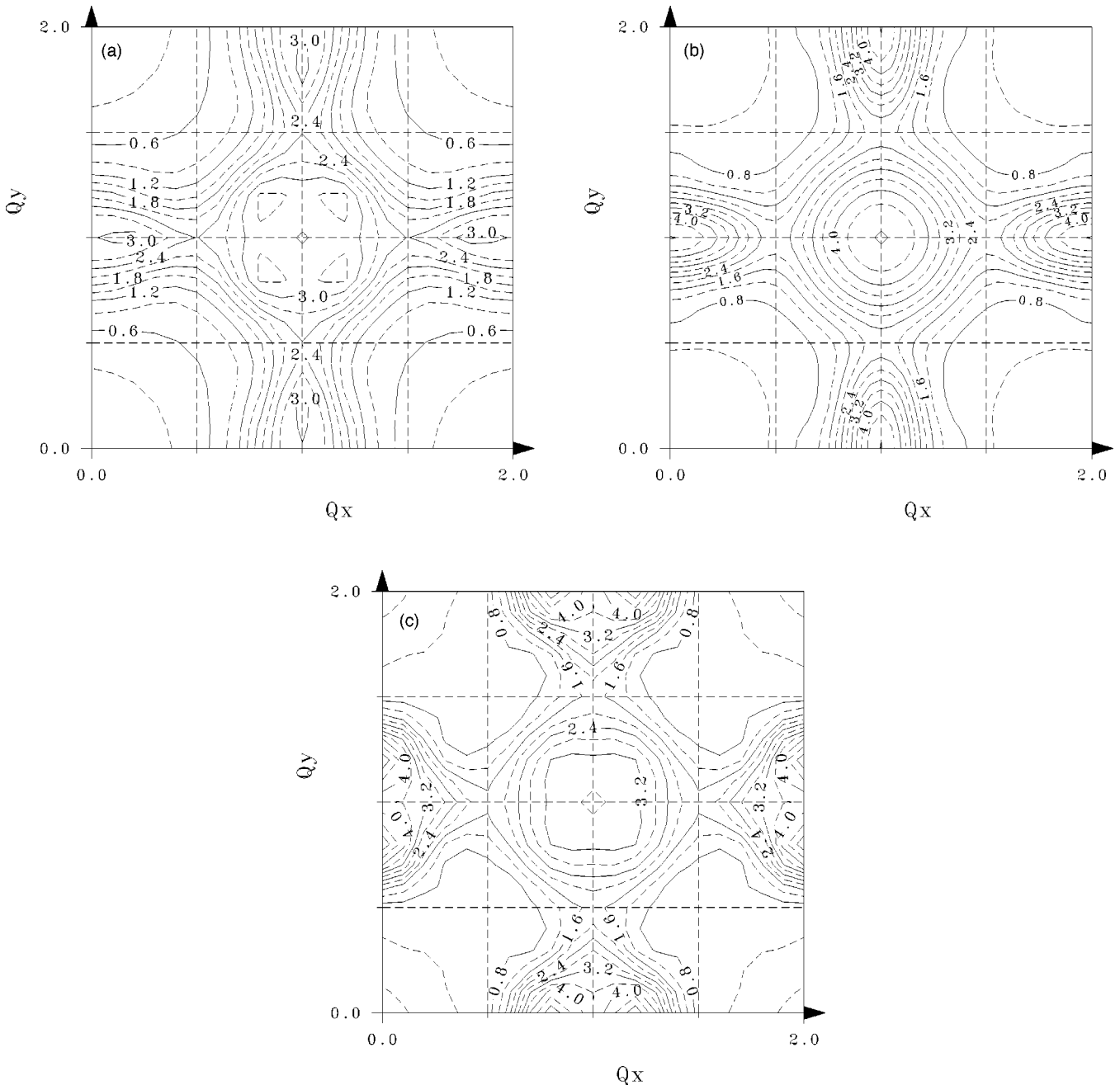

FIG. 4. Simulated SRO in Pt-V by Monte Carlo simulation in (a) Pt_2V, (b) Pt_3V, and (c) Pt_8V, in the (100) plane. For those simulations, we used the same EPI set obtained by inverse Monte Carlo simulation from the SRO of Pt_3V.

is the signature of long range interactions. Indeed, long-range oscillating $V(\vec{R})$, as those due to Fermi surface nesting, lead almost inevitably to incommensurate locations of the $\alpha(\vec{q})$ maxima, which may vary continuously with concentration or temperature. This is probably the case of some Cu-based alloys.[13–17] In our case, the $V(\vec{R})$ are indeed incommensurate, but they do not seem long ranged. More precisely, if we try to fit them with a law of the form $\cos(\vec{k}\cdot\vec{r})/r^n$, the best fit is obtained for $n=3$, and fits with $n=1$ or $n=2$ are pretty bad. This seems to exclude Fermi surface nesting effects. In fact, incommensurate, or even long-range interactions are not prerequisites to get an incommensurate $\alpha(\vec{q})$. An adequate competition between the $V(\vec{R})$ is sufficient. For instance, in the simple case $V_1=100$, $V_2=8$, $V_8=2$, $V(\vec{q})$ exhibits a commensurate minimum at $\langle 1\frac{1}{2}0\rangle$, whereas the $\alpha(\vec{q})$ maxima are incommensurate, and splitted around $\langle 1\frac{1}{2}0\rangle$. On heating, they shift towards $\langle 1\frac{1}{2}0\rangle$.

B. Concentration dependence of the EPI in Ni-V

As in the Pt-V system, the SRO pattern in the Ni-V system is sensitive to the concentration as well, but this concentration sensitivity has a different origin. Contrary to the Pt-V system, the EPI's in Ni-V significantly depend on the concentration (see Fig. 3). For example, the sign of V_2 changes from Ni_2V to Ni_8V. The SRO variations in Ni-V are mainly due to *c*-dependent EPI. In the Ni-V system, it seems that we

TABLE I. Ground states and transition temperatures calculated from EPI determined in the disordered phase of the alloy in the Pt-V and Ni-V systems. We note that, for Pt_2V, the predicted ground state [phase 22 in the Kanamori nomenclature (Ref. 22)] differs from the observed one (the Pt_2Mo-like phase), but the calculated energy difference is very small (≈ 9 meV).

$Pt_{1-c}V_c$	$c=\frac{1}{9}$	$c=\frac{1}{4}$	$c=\frac{1}{3}$
Ground state	A_8B	DO_{23}	22
and calculated T_c	$T_c^{cal}\sim 850$ K	$T_c^{cal}\sim 1100$ K	$T_c^{cal}\sim 500$ K
Experimental ground state	A_8B	DO_{22}	Pt_2Mo
and T_c^{exp}	$T_c^{exp}=1090$ K	$T_c^{exp}=1288$ K	$T_c^{exp}=1373$ K
$Ni_{1-c}V_c$	$c=\frac{1}{9}$	$c=\frac{1}{4}$	$c=\frac{1}{3}$
Ground state	A_8B	DO_{22}	Pt_2Mo
and calculated T_c	$T_c^{cal}\sim 500$ K	$T_c^{cal}=1113$ K	$T_c^{cal}\sim 680$ K
Experimental ground state	A_8B	DO_{22}	$'Pt_2Mo'$
and T_c^{exp}	$T_c^{exp}\sim 678$ K	$T_c^{exp}=1318$ K	$T_c^{exp}=1193$ K

measured the *c*-dependent EPI as expected on grounds of electronic structure calculations.

C. Properties deduced from the EPI

We display in Table I the ground states obtained with our sets of interactions and the corresponding transition temperatures, as calculated by Monte Carlo simulations. Except for the A_2B stochiometry, we obtain an overall agreement with the experimental data. In particular, the fact that, for Ni_8V and Pt_8V, we find the correct ground states is a strong indication of the relevance of the long-range part of our interaction sets. Indeed, with only four interactions, the ground state at composition $c=\frac{1}{9}$ is degenerate among many A_8B structures.[22] The longest-ranged EPI we found lift precisely this degeneracy in favor of the experimentally observed structure.

We note that, for Pt_3V, the ground state is predicted to be DO_{23} instead of the experimentally observed DO_{22} phase. However, the calculated energy difference between DO_{23} and DO_{22} is very small (-3.3 meV per site). More generally, we find that all the L_{12}-based long period structures are almost degenerate with DO_{23}. This is in agreement with the experimental observation of these long period structures in the pseudobinary alloys $PtV-(Ti,Rh)$,[23] which should be mainly understood as a symptom of quasidegeneracy.

V. DISCUSSION

However, this *qualitative* agreement goes together with a *quantitative* discrepancy with electronic structure calculations (LMTO). The latter, based on *ordered* structures, lead to $\Delta E(L1_2-DO_{22})=65$ meV,[23,24] whereas we find only 2 meV by our method, which relies on measurements in the *disordered* state. For Ni_3V, we already pointed out the same type of discrepancy between our approach based on the experiment and *ab initio* calculations.[25,10] It had been suggested that this discrepancy could be partially attributed to electronic excitations.[10,26] However, as the Sommerfeld approximation was used, this effect was overestimated. Since, Wolverton and Zunger[1] have performed a more accurate calculation, showing that the first principles ΔE, which is around 100 meV at $T=0K$, decreases only by 27% at 1400 K if the electronic and magnetic excitations are taken into account. Phonon excitation can also be suspected to explain that discrepancy, but, for Pd_3V, which is very similar to our compounds, Van de Walle *et al.*[28] have estimated a phonon entropy difference to $0.08\ K_B$/atom, which corresponds only to a free energy difference of 10 meV at the temperature of our diffuse scattering measurements, i.e., 1400 K. Other more complicated effects cannot be completely excluded, but the simplest explanation is to assume that the EPI are sensitive to the degree of order,[27] through an obvious blurring of the density of states (DOS) upon disordering. This effect is expected to be particularly important for the $L1_2$ structure of our alloys, which shows a strong DOS peak at the Fermi level, in both ferromagnetic and nonmagnetic states.[29] A KKR-CPA calculation has been performed by Johnson[29] on Ni_3V. For the fully ordered state of Ni_3V, he recovers the ΔE value obtained by LMTO but, in the disordered state, ΔE is found to be close to the values we deduced from our measurements. These facts are strong indications of the validity of his method.

The simulated values of the transition temperatures are generally about 200 K below the experimental values, except for Ni_2V and Pt_2V. For the latter compounds, the experimental T_c's are at least twice the simulated ones (see Table I). The same kind of discrepancy has already been encountered in Ni_2Cr.[5] This could be directly linked to the particular structure of the ground state found in these three A_2B compounds. Their common ''Pt_2-Mo'' ordered structure is built on a periodic stacking of pure (110) planes, two of *A* atoms followed by one of *B* atoms. That strong local inhomogeneity, which is very different from the disordered state, could explain why it is difficult to reproduce properties of the *ordered* state from EPI determined in the *disordered* phase. Calculations analogous to those performed by Johnson[29] on Ni_3V should probably solve this problem.

VI. CONCLUSION

To conclude, for the Pt-V system, we found *c*-independent EPI, despite drastic changes of the SRO topology with concentration. We found the same *c* independence of the EPI for the Ni-Cr system. This situation contradicts elementary arguments of electronic structure. The Ni-V system is less paradoxical to that extent. On the other hand, together with a qualitative agreement, we found quantitative

discrepancies between properties deduced from our measurements in the *disordered* state, and the electronic structure calculations, if performed in the *ordered* state. These discrepancies are most probably due to the local order dependence of the EPI. They are likely to be solved by calculations which are able to handle the degree of order, like the KKR-CPA calculations.[29]

ACKNOWLEDGMENTS

The authors would like to thank D. Regen (ONERA Châtillon) for the high-quality single crystals.

APPENDIX

As explained above, we need a simple and direct expression of $\alpha(\vec{q})$, as a function of the $V(\vec{R})$'s, that goes beyond the KCM formula. We present below a very simple derivation of such an expression.

The usual mean field theory, on which the KCM formula relies, is based on the equation

$$\langle \sigma_n \rangle = \tanh\left[\beta \left(h_n - \sum_{p \neq n} V_{np} \langle \sigma_p \rangle \right) \right], \tag{A1}$$

where $\beta = (kT)^{-1}$ and h_n is the local field applied at site n. In this framework, the estimate of the susceptibility $\chi_{mn} = \partial \langle \sigma_n \rangle / \partial h_m$ includes not only the influence of h_m on $\langle \sigma_n \rangle$, which is mediated through the lattice by any sequence of sites $(p,q, \ldots)$ which link, via the interactions V_{pq}, the site n and m, but also the effect of this prior modification of $\langle \sigma_n \rangle$ on all the sites $p \neq n$. The change of magnetization on these sites induce an unwanted variation on $\langle \sigma_n \rangle$. The way to get rid of this stray effect is to compute the effective field at site $p (p \neq n)$ in the assumption that there is no spin on site n, or, equivalently, to apply to each $\langle \sigma_p \rangle$ a correction which annihilates the unwanted effect of $\langle \sigma_n \rangle$. In the spirit of a high-temperature expansion, the correction, which must be subtracted, is the local susceptibility at site p: $\partial \langle \sigma_p \rangle / \partial h_p$, multiplied by the contribution of $\langle \sigma_n \rangle$ to the molecular field at p, i.e., $-V_{np} \langle \sigma_n \rangle$. Contrary to the Onsager cavity approach,[32] this correction is applied prior to the use of the fluctuation-dissipation theorem. Once corrected, Eqn. (A1) becomes

$$\langle \sigma_n \rangle = \tanh \beta \left(h_n - \sum_{p \neq n} V_{np} [\langle \sigma_p \rangle + \beta (1 - \langle \sigma_p \rangle^2) V_{np} \langle \sigma_n \rangle] \right). \tag{A2}$$

Using the fluctuation-dissipation theorem on Eq. (A2), we obtain, in the Fourier space and for the disordered state

$$\alpha(\vec{q}) = \frac{1}{1 + \Lambda + 4\beta c(1-c) \tilde{V}(\vec{q})}, \tag{A3}$$

where $\tilde{V}(\vec{q})$ is the Fourier transform of $\tilde{V}(\vec{R})$ defined by

$$\tilde{V}(\vec{R}) = V(\vec{R}) \{ 1 - 2(1-2c)^2 \beta V(\vec{R}) \} \tag{A4}$$

with

$$\Lambda = 16 \beta^2 c^2 (1-c)^2 \sum_{\vec{R}} V^2(\vec{R}). \tag{A5}$$

Equation (A4) shows that the interaction $V(\vec{R})$, if positive, is more attenuated when $V(\vec{R})$ itself is large, when the temperature is low, and when the concentration is far from $c = \frac{1}{2}$.

The more important feature of the above results is that they lead to a simple and direct expression for $\alpha(\vec{q})$. Analytical expressions of $\alpha(\vec{q})$ are also obtained within the gamma expansion method,[20,21] the ring approximation,[30] or the alpha expansion method,[31] but these expressions are not direct, as they contain a parameter (the diagonal part of the self-energy), which must be determined self-consistently by requiring that the sum rule $\Sigma_{\vec{q}} \alpha(\vec{q}) = N$ be fulfilled. Meanwhile, it is easy to show that the present expression of $\alpha(\vec{q})$ is equivalent, up to the second order in $1/T$, to the ring approximation.[30] Finally, we note that the same expression of $\alpha(\vec{q})$ has been obtained independently by Tsatskis[31] through a more formal and systematic high-temperature expansion.

The above expressions (A3)–(A5) for $\alpha(\vec{q})$ easily explain the c-behavior of the SRO topology. In the Pt-V case, the scaling of Eq. (A4) will mainly reduce the strongest interactions, i.e., V_1, and this for the lowest vanadium concentrations. The SRO will be then dominated by further EPI and will in general be incommensurate. That is the case in Pt_8V, where the diffuse maxima appear at incommensurate positions along the $\langle h00 \rangle$ line.

On the other hand, for higher vanadium concentration, the renormalization of V_1 will be negligible. The dominance of V_1 will yield, at high temperature, a standard KCM behavior, i.e., a large intensity ridge $\alpha(\vec{q})$ along the $\langle 1k0 \rangle$. The exact position of the maximum along that ridge is dictated by the interactions $V(i); i \geq 2$. That is the case of Pt_2V where a flat diffuse intensity is measured along the $\langle 1k0 \rangle$ with small maxima in the same direction (Fig. 1). At lower temperatures, the intensity on (100) should increase much faster that on other points and this should lead to a shift of the maximum along the $\langle 1k0 \rangle$ line, towards the (100) point.[7]

*Present address: European Synchrotron Radiation Facility, BP 220, F-38043 Grenoble, France.

[1] C. Wolverton, and A. Zunger, Phys. Rev. B **52**, 8813 (1995).

[2] D.D. Johnson, J.B. Staunton, and F.J. Pinski, Phys. Rev. B **50**, 1475 (1994).

[3] B. Schönfeld, L. Reinhardt, and G. Kostorz, Phys. Status Solidi B **147**, 457 (1988).

[4] W. Schweika and H.G. Haubold, Phys. Rev. B **37**, 9240 (1988).

[5] R. Caudron, M. Sarfati, M. Barrachin, A. Finel, F. Ducastelle, and F. Solal, J. Phys. I **2**, 1145 (1992).

[6] D. Le Bolloc'h, T. Cren, R. Caudron, and A. Finel, Comput. Mater. Sci. **8**, 24 (1997).

[7] D. Le Bolloc'h, R. Caudron, and A. Finel, Phys. Rev. B **57**, 2801 (1998).

[8] D. Schryvers, Ph.D. thesis, Wilrijk, 1985.

[9] Hansen, *Constitution of Binary Alloys* (McGraw Hill, New York, 1958.

[10] M. Barrachin, A. Finel, R. Caudron, A. Pasturel, and A. Francois,

Phys. Rev. B **50**, 12 980 (1994).
[11] F. Solal, R. Caudron, F. Ducastelle, A. Finel, and A. Loiseau, Phys. Rev. Lett. **58**, 2245 (1987).
[12] C.J. Sparks and B. Borie, in *Local Atomic Arrangements Studied by X-Ray Diffraction*, edited by J.B. Cohen and J.E. Hilliard (Gordon and Breach, New York, 1966).
[13] L. Reinhardt, B. Schönfeld, G. Kostorz, and W. Bürer, Phys. Rev. B **41**, 1727 (1990).
[14] J.M. Cowley, J. Appl. Phys. **21**, 24 (1950); S.C. Moss, *ibid.* **35**, 3547 (1964); P. Bardhan and J.B. Cohen, Acta Crystallogr., Sect. A: Cryst. Phys., Diffr., Theor. Gen. Crystallogr. **32**, 597 (1976); B.D. Butler and J.B. Cohen, J. Appl. Phys. **65**, 2214 (1989).
[15] H. Reichert, S.C. Moss, and K.S. Liang, Phys. Rev. Lett. **77**, 4382 (1996).
[16] J. Kulik, D. Gratias, and D. De Fontaine, Phys. Rev. B **40**, 8607 (1989).
[17] R.O. Scattergood, S.C. Moss, and M.B. Bever, Acta Metall. **18**, 1087 (1970); H. Chou, S.M. Shapiro, and S.C. Moss, Phys. Rev. B **42**, 500 (1990); H. Roelofs *et al.*, Scr. Mater. **34**, 1393 (1996); B. Schönfeld *et al.*, Acta Mater. **44**, 335 (1996).
[18] Magnetic SRO could not influence the diffuse intensity at the experimental temperature ($T=774$ K) since Ni_8V becomes paramagnetic at 10 K if we extrapolate the existing data (see Ref. 9).
[19] S.C. Moss and P.C. Clapp, Phys. Rev. **171**, 764 (1968).
[20] V.I. Tokar, Phys. Rev. Lett. **110A**, 453 (1985).
[21] V.I. Tokar, I.V. Masanskii, and T.A. Grishchenko, J. Phys.: Condens. Matter **2**, 10 199 (1990); I.V. Masanskii, V.I. Tokar, and T.A. Grishchenko, Phys. Rev. B **44**, 4647 (1991).
[22] J. Kanamori and Y. Kakehashi, J. Phys. (France) **38**, C7-274 (1977).
[23] E. Cabet, A. Pasturel, F. Ducastelle, and A. Loiseau, Phys. Rev. Lett. **76**, 3140 (1996).
[24] Rosengaard and H.L. Skriver, Phys. Rev. B **50**, 4848 (1994).
[25] A. Finel, M. Barrachin, R. Caudron and A. Francois, in *Metallic Alloys: Experimental and Theoretical Perspectives*, edited by J.S. Faulkner and R.J. Jordan, Vol. 256 of *NATO Advanced Study Institute, Series E: Applied Sciences* (Kluwer, Boston, 1994), p. 215, conference held in July 1993.
[26] C. Wolverton, A. Zunger, and Z.-W. Lu, Phys. Rev. B **49**, 16 058 (1994).
[27] D. Le Bolloc'h, Ph. D. thesis, University of Rennes, 1997.
[28] A. van de Walle and G. Ceder, Phys. Rev. B **61**, 5972 (2000).
[29] D. Johnson (unpublished).
[30] R.V. Chepulskii and V.N. Bugaev, J. Phys.: Condens. Matter **10**, 7309 (1998).
[31] I. Tsatskis, in *Local Structure from Diffraction, Fundamental Materials Science Series*, edited by M.F. Thorpe and S.J.L. Billings (Plenum, New York, 1998).
[32] L. Onsager, J. Am. Chem. Soc. **58**, 1468 (1936).